



**HAL**  
open science

## Influential parameters on electromagnetic properties of nickel-zinc ferrites for antenna miniaturization

David Souriou, Jean-Luc Mattei, Alexis Chevalier, Patrick Queffelec

► **To cite this version:**

David Souriou, Jean-Luc Mattei, Alexis Chevalier, Patrick Queffelec. Influential parameters on electromagnetic properties of nickel-zinc ferrites for antenna miniaturization. *Journal of Applied Physics*, American Institute of Physics, 2010, 107, pp.09A518. 10.1063/1.3356235 . hal-00488880

**HAL Id: hal-00488880**

**<https://hal.univ-brest.fr/hal-00488880>**

Submitted on 6 Jun 2016

**HAL** is a multi-disciplinary open access archive for the deposit and dissemination of scientific research documents, whether they are published or not. The documents may come from teaching and research institutions in France or abroad, or from public or private research centers.

L'archive ouverte pluridisciplinaire **HAL**, est destinée au dépôt et à la diffusion de documents scientifiques de niveau recherche, publiés ou non, émanant des établissements d'enseignement et de recherche français ou étrangers, des laboratoires publics ou privés.

## Influential parameters on electromagnetic properties of nickel–zinc ferrites for antenna miniaturization

David Souriou,<sup>a)</sup> Jean-Luc Mattei, Alexis Chevalier, and Patrick Queffelec

*Laboratoire des Sciences et Techniques de l'Information, de la Communication et de la Connaissance (Lab-STICC), UMR CNRS 3192, Université Européenne de Bretagne–U.B.O., 6 avenue Le Gorgeu, CS 93837, 29238 Brest Cedex 3, France*

(Presented 20 January 2010; received 27 October 2009; accepted 1 December 2009; published online 6 May 2010)

Electromagnetic properties of nickel–zinc ferrites based materials make them potential candidates for applications linked to telecommunications. In the present study, nanosized particles of spinel ferrite  $\text{Ni}_{0.5}\text{Zn}_{0.3}\text{Co}_{0.2}\text{Fe}_2\text{O}_4$  were prepared by coprecipitation method. An optimized material is obtained after adequate heat treatment and partial filling of the porosity by epoxy resin. This material lies between ceramic and composite medium (with porosity close to 40%), and shows almost constant complex permeability and permittivity in the frequency range from 0.1–0.7 GHz, and equal to  $\sim 3.5-j0.15$  (loss tangent  $\sim 0.04$ ) and  $\sim 4-j0.2$  (loss tangent  $\sim 0.02$ ), respectively. The refractive index  $n$  is close to 3.75. These electromagnetic properties, in particular the low levels of losses, show that this material could be useful to the design of miniaturized antennas in the VHF-uhf (300–700 MHz) range of frequency. © 2010 American Institute of Physics.

[doi:10.1063/1.3356235]

### I. INTRODUCTION

The tremendous development of handheld terminals in the low uhf range (300–700 MHz) asks for antennas of reduced physical dimension without affecting their electromagnetic performances.<sup>1–4</sup> Actually, present antennas are too large to allow satisfactory integration into such devices, and the present techniques used to reduce their size degrade the performances of the antennas.<sup>5</sup> Materials with low dielectric and magnetic loss tangents are very useful to the design of miniaturized antennas and simultaneously maintaining the electrical dimensions (the electrical length is the product between the geometrical length of the medium with its refractive index). Actually, materials that show sufficiently low magnetic and dielectric loss tangents ( $\text{tg}\delta_\mu = \mu''/\mu'$  and  $\text{tg}\delta_\epsilon = \epsilon''/\epsilon' < 5 \times 10^{-2}$ ) and a refractive index ( $n = \sqrt{\mu'\epsilon'}$ ) large enough, could be useful to the design of antennas with reduced physical dimensions ( $\mu'$  and  $\epsilon'$  are real parts of relative permeability and permittivity, respectively, and  $\mu''$  and  $\epsilon''$  are the imaginary parts). To achieve low-loss requirement, the material must have a resonant frequency far from the desired frequency band. Co-substituted NiZn ferrites are promising magnetic materials for radiofrequency applications, i.e., upto 300 MHz.<sup>6</sup> Recent studies show results for antenna miniaturization at lower frequencies.<sup>2,3,7</sup> However, it is not usual to use spinel ferrites for microwave devices. Our task is concerned with soft magnetic material-spinel ferrite that would show potentiality to be used in the frequency range 300–0.7 GHz.

This paper will show how the electromagnetic properties of the final substrate are influenced—for the chosen composition—by the heat treatment (calcination and sintering) and also by filling of the porosity of the sample.

### II. EXPERIMENTAL PROCEDURE

Ni–Zn–Co ferrites nanopowders of composition  $\text{Ni}_{0.5}\text{Zn}_{0.3}\text{Co}_{0.2}\text{Fe}_2\text{O}_4$  (labeled J2 powder) were prepared via the conventional coprecipitation method.<sup>8</sup>

First high purity raw materials, nickel chloride, cobalt chloride, zinc chloride, and iron (III) chloride were taken from their molar solution in accurate stoichiometric proportions. These solutions were poured into boiling solution of NaOH (0.45 mol/l) under stirring ( $\sim 350$  rpm). After coprecipitation, pH is set between 11.5 and 12, which we found to be the optimum pH for stoichiometric precipitation. Reaction is continued for 30 min at temperature 100 °C, the suspension is cooled to ambient temperature and is then centrifuged at 6000 rpm for 13 min after sedimentation. The residue is dried in an electrical oven before to be calcinated (temperature  $T_c = 650$  or 800 °C) in air for 3 h (with heating and cooling rates of 200 °C/h) to obtain a ferrite powder. The average particle size was 25 nm before the calcination stage (transmission electron microscopy observation). The density of the powder is measured by a helium pycnometer.

Then this powder was compacted by uniaxial pressing (applied pressure: 325 MPa) into a toroidal shape, chosen for its convenience for electromagnetic characterization by using the coaxial line-based method. The final ferrite body was obtained after sintering in air (temperature  $T_s = 900$  or 1000 °C) for 1 h at a heating rate of 300 °C/h and were subsequently cooled at a cooling rate of 600 °C/h to room temperature. These temperature profiles were optimized with the help of differential thermal analysis. The density of our samples is determined by measurement of their dimensions (results shown in Table I).

A Hewlett Packard HP 8753ES network analyzer setup was used for the measurements of the sample parameters  $\epsilon$  (complex permittivity  $\epsilon' - j\epsilon''$ ) and  $\mu$  (complex permeability  $\mu' - j\mu''$ ) over a wide range of frequencies (10 MHz–6 GHz).

<sup>a)</sup>Electronic mail: souriou.david@wanadoo.fr.

TABLE I. Samples density as a function of heat treatments (powder density, 5.113 g cm<sup>-3</sup>).

Calcination temperature (°C)	Sintering temperature (°C)	Density (%)
650	900	73.12
800	900	57.34
650	1000	87.71

### III. RESULTS AND DISCUSSION

#### A. Influence of the temperature of calcination

##### 1. Calcination of the green body

Real and imaginary parts of permeability and permittivity of two J2 samples (calcinated at  $T_C=650$  °C and 800 °C, respectively) show the sensitivity of the electromagnetic properties to the value of  $T_C$  [Figs. 1(a) and 1(b)]. The main result is a drastic decrease in dielectric losses between 650 and 800 °C. A slight (10%) increase of  $\mu'$  below 1 GHz is associated to a shift of  $\mu''$  to lower frequencies as expected from Snoek's law.<sup>9</sup>

##### 2. Influence on the calcination temperature on sintering

Both J2 samples were sintered at  $T_S=900$  °C [Figs. 2(a) and 2(b)]. Here two salient results are underlined. First, whatever the value of  $T_C$  the real permeability of both samples reaches a same value after sintering. Second, the real permittivity of the sample calcinated at  $T_C=800$  °C re-

mains unchanged by sintering at  $T_S=900$  °C, whereas that of the sample calcinated at  $T_C=650$  °C is strongly decreased.

These experimental data can be roughly understood as follows. For a calcinating process that occurs at  $T_C=800$  °C, the sintering process actually starts, then a network of necks of matter between grains is achieved.<sup>10</sup> This leads to a more heterogeneous grain size distribution. Consequently, the resonance peak is broader and the magnetic losses higher at lower frequencies. Owing the aimed applications,  $T_C=650$  °C is the calcination temperature that will be held.

#### B. Influence of the sintering temperature

Starting from J2 powder previously calcinated at 650 °C, two samples were sintered at  $T_S=900$  °C and  $T_S=1000$  °C, respectively. The real part of permeability increases with the sintering temperature [Fig. 3(a)], whereas the maximum of  $\mu''$  shift to low frequency according to Snoek's law again.<sup>9</sup> The densification by sintering occurs in three steps as follows: bridge formation between grains, granular rearrangement, and then grain growth.<sup>10</sup> The width of the resonance peak is notably increased by high sintering temperature (1000 °C), this can be linked to grain growth. The observed decreases of  $\epsilon'$  and  $\epsilon''$  with increasing  $T_S$  [Fig. 3(b)] is also a marker of a reduced porosity. Dielectric losses are appreciably reduced when  $T_S=1000$  °C, due to a shrinkage of porosity that decreases area effects.

Low magnetic losses and satisfactory optical index are then obtained with J2 powder calcinated at  $T_C=650$  °C and

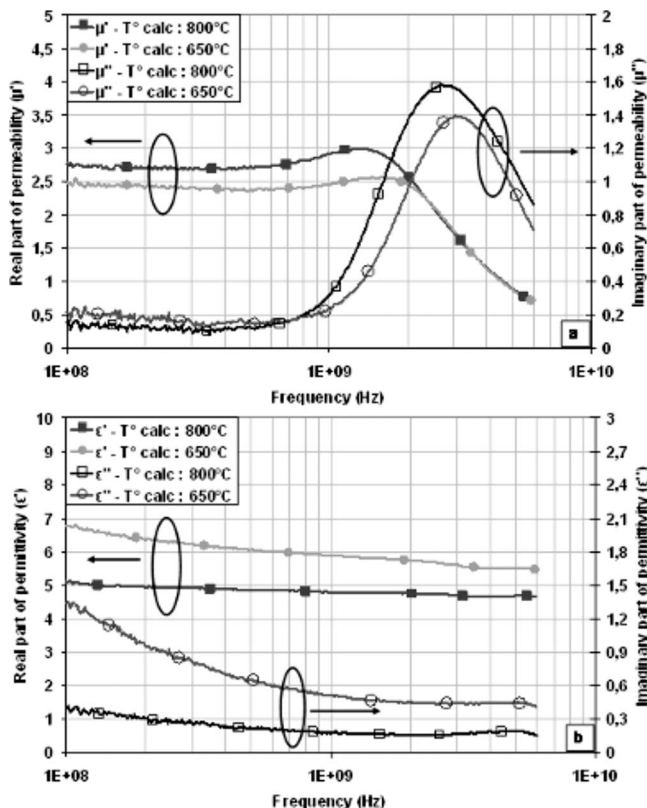
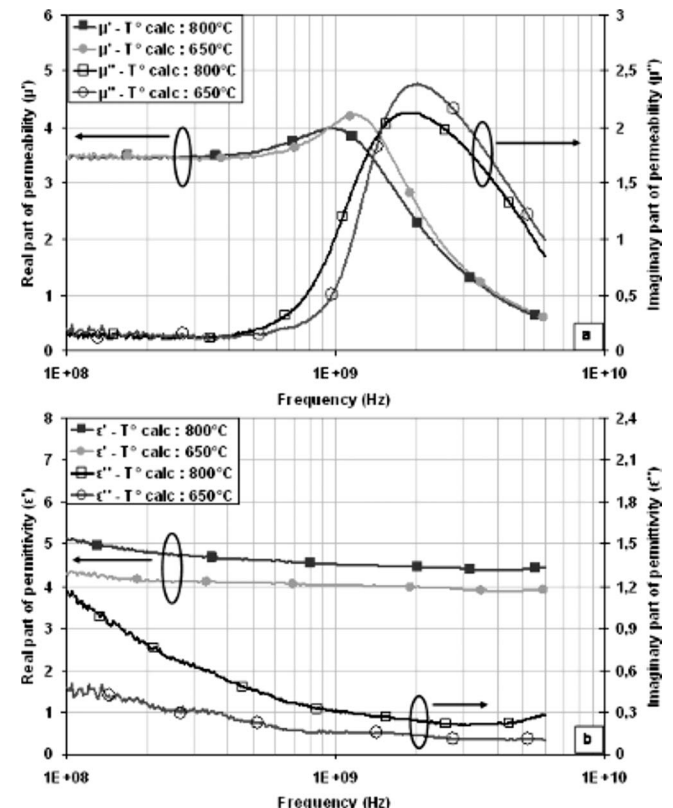


FIG. 1. Measured permeability (a) and permittivity (b) spectra of the calcinated green body.

FIG. 2. Measured permeability (a) and permittivity (b) spectra after calcination and sintering ( $T_S=900$  °C).

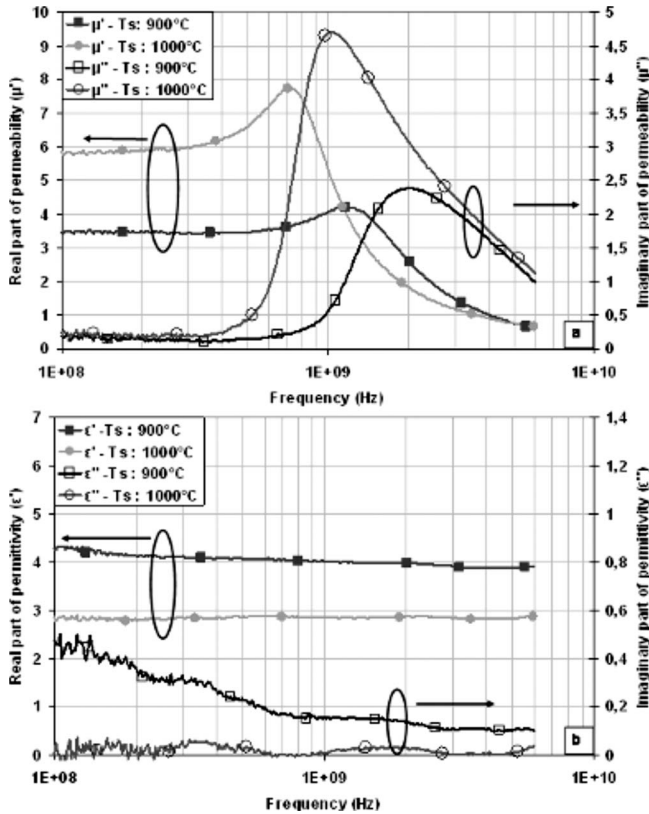


FIG. 3. Measured permeability (a) and permittivity (b) spectra after calcination at 650 °C and sintering.

sintered at  $T_S=900$  °C. However, dielectric losses  $tg\delta_{\epsilon'}$  remain too high for the envisaged applications.

**C. Influence of soaking**

In order to get a reduced  $tg\delta_{\epsilon'}$ , the samples are afterwards immersed into a solution of epoxy resin dissolved in acetone and dried. A fraction of voids is filled by the resin, and the global porosity of the sample is lowered (Table II). The measured permittivity and permeability are shown on Fig. 4. A noteworthy fall down of  $\epsilon''$  promotes the so obtained material as a suitable one for antenna miniaturization in the frequency range 100–700 MHz.

**IV. CONCLUSION**

Our experiments have shown that electromagnetic properties of ferrites are influenced by several parameters. For a nanometric powder elaborated by coprecipitation, the calcination and the sintering temperatures must be chosen so that the final material fits desired electromagnetic requirements for the reduction of antenna size.

The heat treatment submitted to the studied ferrite powders leads to a porous material with high ferrite content that

TABLE II. Measured electromagnetic parameters (frequency range 100–700 MHz) after soaking with epoxy resin (amount of filled porosity: 21%).

	$tg\delta_{\epsilon}=\epsilon''/\epsilon'$	$tg\delta_{\mu}=\mu''/\mu'$	$\sqrt{\mu'\epsilon'}$
Before soaking	0.043–0.115	0.054–0.067	3.75–3.90
After soaking	0.015–0.046	0.048–0.064	3.64–3.75

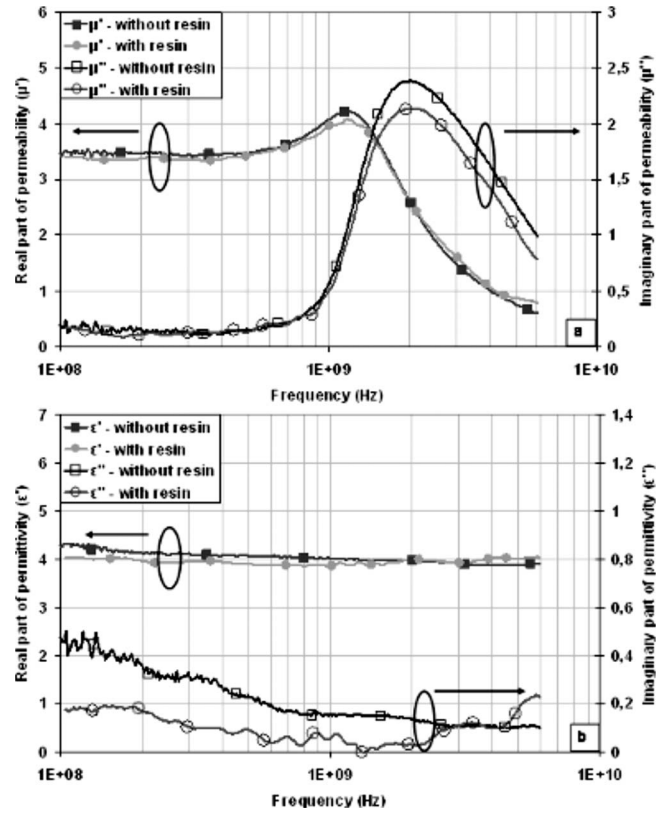


FIG. 4. Measured permeability (a) and permittivity (b) spectra after heat treatment ( $T_C=650$  °C,  $T_S=900$  °C) followed by soaking with epoxy resin.

can be considered to lie in the intermediate state between the sintered ferrite and the composite. Then, we take advantage of the composite character of the obtained ceramic sample to get ferrite with satisfactory permeability and permittivity levels at unusual high resonance frequency for soft ferrites.

A striking point in the presented data is the low level of magnetic (and dielectric) loss tangents on a wide frequency range, which clearly distinguish our results.

**ACKNOWLEDGMENTS**

This work was supported by the Agence Nationale pour la Recherche (ANR-NAOMI project).

<sup>1</sup>H. Mosallaei and K. Sarabandi, *IEEE Trans. Antennas Propag.* **52**, 1558 (2004).  
<sup>2</sup>S. Bae, Y. K.Hong, and A. Lyle, *J. Appl. Phys.* **103**, 07E929 (2008).  
<sup>3</sup>I. Kim, S. Bae, and J. Kim, *J. Korean Phys. Soc.* **52**, 127 (2008).  
<sup>4</sup>K. Buell, H. Mossallaei, and K. Sarabandi, *IEEE Trans. Microwave theory Tech.* **54**, 135 (2006).  
<sup>5</sup>J. Holopainen, J. Villanen, M. Kyro, C. Icheln, and P. Vainikainen, Antenna Technology Small Antennas and Novel Metamaterials, Proceedings of IEEE International Workshop, March 6–8, 2006 (unpublished), pp.305–308.  
<sup>6</sup>R. Lebourgeois, J. Ageron, H. Vincent, and J.-P. Ganne, Proceedings of the ICF, Vol. 8, Kyoto (Japan) (2000), p. 373.  
<sup>7</sup>L. Z. Wu, J. Ding, H. B. Jiang, C. P. Neo, L. F. Chen, and C. K. Ong, *J. Appl. Phys.* **99**, 083905 (2006).  
<sup>8</sup>P. Mathur, A. Thakur, and M. Singh, *J. Magn. Magn. Mater.* **320**, 1364 (2008).  
<sup>9</sup>A. N. Lagarkov and K. N. Rozanov, *J. Magn. Magn. Mater.* **321**, 2082 (2009).  
<sup>10</sup>R. Valenzuela, “*Magnetic Ceramics*” (Cambridge University Press, Cambridge, UK, 1994).